Recent advances in quantum dot physics / Nouveaux développements dans la physique des boîtes quantiques

Intersublevel transitions in self-assembled quantum dots

Philippe Boucaud [*], Sébastien Sauvage, Julien Houel

Institut d'Electronique Fondamentale, CNRS Université Paris-Sud XI, bâtiment 220, 91405 Orsay cedex, France

Available online 13 November 2008

Abstract

Intersublevel transitions in semiconductor quantum dots are transitions of a charge carrier between quantum dot confined states. In InAs/GaAs self-assembled quantum dots, optically active intersublevel transitions occur in the mid-infrared spectral range. These transitions can provide a new insight on the physics of semiconductor quantum dots and offer new opportunities to develop mid-infrared devices. A key feature characterizing intersublevel transitions is the coupling of the confined carriers to phonons. We show that the effect of the strong coupling regime for the electron–optical phonon interaction and the formation of mixed electron–phonon quasi-particles called polarons drastically affect and control the dynamical properties of quantum dots. The engineering of quantum dot relaxation rates through phonon coupling opens the route to the realization of new devices like mid-infrared polaron lasers. We finally show that the measurement of intersublevel absorption is not limited to quantum dot ensembles and that the intersublevel ultrasmall absorption of a single quantum dot can be measured with a nanometer scale resolution by using phonon emission as a signature of the absorption. ***To cite this article: P. Boucaud et al., C. R. Physique 9 (2008).***
© 2008 Académie des sciences. Published by Elsevier Masson SAS. All rights reserved.

Résumé

Transitions inter-sous-niveaux dans les boîtes quantiques auto-assemblées. Les transitions inter-sous-niveaux dans les boîtes quantiques de semi-conducteurs sont les transitions que peut effectuer un porteur de charge entre niveaux confinés. Dans les boîtes quantiques auto-assemblées InAs/GaAs, les transitions inter-sous-niveaux optiquement actives peuvent être observées dans la gamme spectrale de l'infrarouge moyen. Ces transitions dévoilent de nouvelles facettes de la physique des boîtes quantiques de semi-conducteurs et ouvrent de nouvelles perspectives pour le développement de composants moyen-infrarouges. Une caractéristique clef des transitions inter-sous-niveaux est le couplage des porteurs de charges confinés avec les phonons. Nous montrons que le régime de couplage fort pour l'interaction électron–phonon optique et la formation de particules mixtes électron–phonon appelées polarons gouvernent la dynamique des boîtes quantiques. L'ingénierie des taux de relaxation dans les boîtes quantiques, obtenue au travers du couplage électron–phonon, ouvre la voie à la réalisation de nouveaux dispositifs tels qu'un laser moyen-infrarouge à polarons. Nous montrons enfin que la mesure de l'absorption inter-sous-niveaux n'est pas limitée à des ensembles de boîtes quantiques et que l'absorption ultrafaible d'une boîte quantique unique peut être mesurée avec une résolution spatiale nanométrique en exploitant l'émission de phonons comme signature de l'absorption. ***Pour citer cet article : P. Boucaud et al., C. R. Physique 9 (2008).***
© 2008 Académie des sciences. Published by Elsevier Masson SAS. All rights reserved.

Keywords: Quantum dots; Intersublevel transitions; Polaron; Mid-infrared

---

[*] Corresponding author.

E-mail addresses: philippe.boucaud@ief.u-psud.fr (P. Boucaud), sebastien.sauvage@ief.u-psud.fr (S. Sauvage), julien.houel@ief.u-psud.fr (J. Houel).

1. Introduction

Self-assembled quantum dots are semiconductor nanostructures which exhibit discrete confined states. A well-known model system is given by InGaAs quantum dots embedded in a GaAs matrix. Soon after the first studies on interband optical transitions in these nanostructures, researchers have started in the mid 1990s to investigate the intersublevel (also called intraband) transitions, i.e. the optical transitions performed by confined charged carriers between conduction states or between valence states. The spectral range covered by these transitions, either bound-to-bound or bound-to-continuum transitions, goes from the mid to the far infrared (wavelength $\lambda \geqslant 3$ µm). A key feature associated with intersublevel transitions is the simplicity of the physics system. The intersublevel transitions can be studied through quantum dots loaded or charged with a single electron on the doubly degenerate ground state. There is no requirement for holes to be present to observe intersublevel absorption. One of the first motivations to study quantum dot intersublevel transitions was to develop new quantum dot infrared photodetectors which were expected to exhibit superior performance as compared to quantum well infrared photodetectors based on intersubband transitions. Independently of these device applications, it has been realized that the study of intersublevel transitions can bring new insight on the quantum dot physics. One of the most significant advance was the observation of the electron–optical phonon strong coupling in this system and the subsequent formation of mixed electron–phonon quasi-particles called polarons. This strong coupling regime has a significant impact on the quantum dot dynamics and it is now well recognized that the coupling between electronic states and the phonons govern many features related to quantum dots. Beyond a deeper analysis of solid-state nanostructures, the tuning of polaron states also provides some tools to engineer the relaxation rates and can lead to the design of novel optical devices. Phonon emission can also be the driving force to observe single quantum dot intersublevel absorption in the mid-infrared spectral range. The purpose of this article is to review the knowledge that has been obtained over the last decade on intersublevel transitions in quantum dots. It is divided in five sections. Section 2 will recall the basic properties of intersublevel absorption of quantum dot ensembles. The electronic structure revealed by the absorption spectra can be compared to the one obtained from three-dimensional modeling using multiband $\mathbf{k} \cdot \mathbf{p}$ formalism. Section 3 will be devoted to the mixed electron–phonon quasi-particles called polarons and their impact on the quantum dot dynamics. Section 4 deals with the infrared emission properties of quantum dots and the possibility to achieve a polaron laser through relaxation rate engineering. Section 5 will finally present recent results on single quantum dot spectroscopy and the observation of single quantum dot ultrasmall absorption with a lateral resolution in the tens of nanometer range much below the diffraction limit.

2. Quantum dot intersublevel absorption and electronic level modeling

Even though a large community of scientists have investigated the self-assembled quantum dots through their interband properties for a long time, the interest of studying intersublevel transitions has also started very early. The first observation of intersublevel absorption in InGaAs self-assembled quantum dots has been reported by Drexler et al. in 1994 [1]. In their studies, the quantum dots were embedded in a MISFET type structure and the loading of electrons into quantum dots was controlled by the voltage applied to a Schottky diode. Far-infrared absorption between the ground and first excited state was reported at low temperature with this technique. Another approach to measure intersublevel transitions is to chemically dope the quantum dots *in situ* during the growth. The carriers can be provided by a silicon modulation doping close to the quantum dot layer. Room temperature electronic bound-to-continuum absorption has been evidenced in a multipass geometry [2]. This bound-to-continuum absorption, essentially polarized along the growth direction, corresponds to transitions between the ground state and the continuum states at an energy equal or larger than the one of the wetting layer states. In the latter case, the polarized absorption was observed in the mid-infrared spectral range between 5 and 12 µm for InGaAs quantum dots. Bound-to-continuum absorption was also observed by photoconductivity measurements at liquid nitrogen temperature [3]. Another approach to observe intersublevel transitions is to perform photo-induced absorption, i.e. by generating carriers which are trapped in the dots using an interband optical pumping [4]. However, the presence of holes can significantly modify the physics of intersublevel transitions, in particular when the dynamical properties are studied.
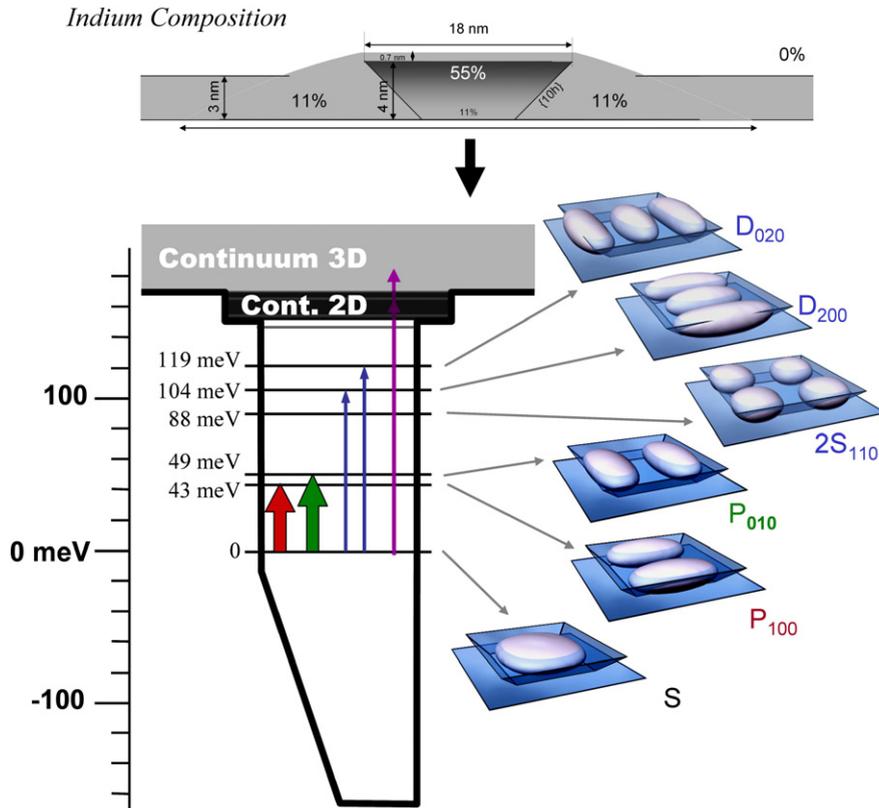
Fig. 1. Electronic structure of a typical InAs/GaAs self-assembled quantum dot. The energies and envelope wave functions are obtained through the three-dimensional resolution of the Schrödinger equation written in 8 band $\mathbf{k} \cdot \mathbf{p}$ formalism and accounting for the geometry and indium composition depicted in the upper part of the figure. The optically allowed transitions are indicated by an arrow.

One of the most investigated intersublevel transitions is the so-called S-P transition between the S ground state (which is spin doubly degenerated), and one of the first excited P states. Standard InGaAs quantum dots epitaxially grown by molecular beam epitaxy exhibit a flat diamond-base shape geometry with a 12% elongation along the [−110] diagonal direction. Recent analysis by transmission electron microscopy has shown that the typical height is 4 nm and the typical base lateral dimensions is 22 nm (diamond diagonal). These values are dispersed throughout the quantum dot distribution by approximatively 12% around the average value. The composition is 40–45% inside the quantum dot, with a vertical gradient down to 30% at the base. This type of geometry leads to an S-P intersublevel absorption resonant around 50–60 meV, i.e. between 20 and 25 μm [5]. Since the confinement of the first two excited states is mainly controlled by the lateral dimensions, the S-P intersublevel absorption is polarized in the layer plane. It can thus be measured in a normal incidence configuration where the light is incident along the [001] growth axis. Because of the quantum dot elongation, the S-P transition is spectrally split into two orthogonally polarized transitions namely the S-P− and S-P+ transitions. The electronic structure of the quantum dot can be calculated by solving in three dimensions the Schrödinger equation written in a multiband $\mathbf{k} \cdot \mathbf{p}$ formalism [6]. Fig. 1 shows a calculated electronic structure along with the associated envelope wavefunctions for the composition depicted in the inset. The transition energy between S and P states is predicted at 43 meV for the [−110] orientation and 49 meV for the [110] direction. The electronic dipole matrix element is 3.7 e.nm for S-P− and 3.4 e.nm for S-P+. The transitions from S to the "D" states at higher energy exhibit a small dipole along the growth axis direction.

The absorption of the S-P transition can be measured using multilayer quantum dot structures. Fig. 2 shows the room temperature typical absorption spectra measured with samples containing 80 quantum dot layers. The layers are separated by 50 nm thick GaAs barriers. The dot density is 4×10^{10} cm^{-2}. The lateral size distribution is ±6% full width at half maximum and translates into a significant inhomogeneous contribution to the spectral width of the polarized absorptions. Note that the absorption results from the first order linear susceptibility of the intersublevel
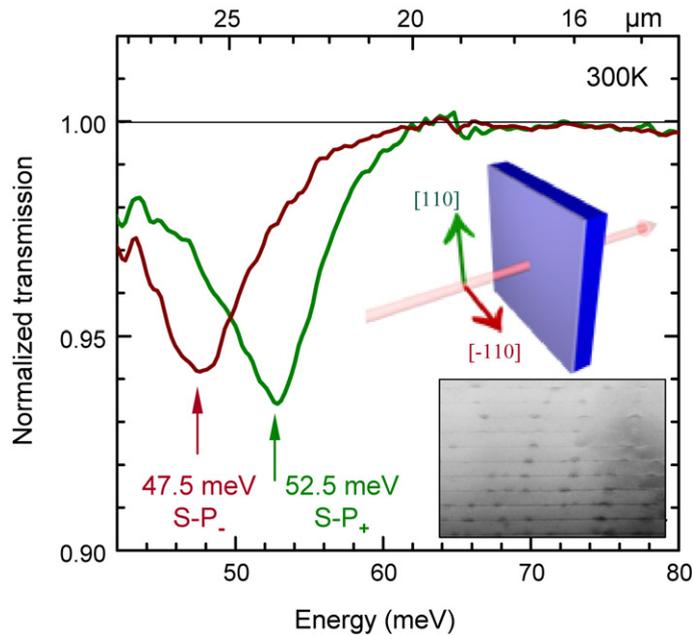
Fig. 2. Transmission of an ensemble of InAs/GaAs self-assembled quantum dots normalized by the transmission of a GaAs substrate of equal thickness. The polarized absorption is reported for a sample containing 80 quantum dot planes separated by 50 nm as illustrated in the Transmission Electron Microscopy image of the inset.

transitions. Second-harmonic and third-harmonic generation in resonance with the conduction S-P-D intersublevel transitions or with the valence intersublevel transitions have also been reported [7,8]. These optical non-linearities also probe the intersublevel energies, dipoles and polarizations, but through higher order of the susceptibility and are very complementary to linear absorption spectroscopy.

3. Quantum dot polaron dynamics

The intersublevel transitions in semiconductor quantum dots cannot be considered as optical transitions between pure electronic states. One has to take into account the coupling to the phonons in order to correctly describe the physics of intersublevel transitions. In polar III-V semiconductors, the carriers are coupled to the optical phonons through the Fröhlich coupling. In GaAs, the longitudinal optical (LO) phonons have a weak dispersion between the zone center and the band edge. In bulk materials or quantum wells, the coupling involves an electronic continuum and the phonon continuum and the interaction remains in the weak coupling regime. The interaction through phonon emission corresponds to an irreversible decay. The situation is quite different in the case of semiconductor quantum dots where the interaction with phonons cannot be treated pertubatively. Discrete states are now coupled to the optical phonon continuum. The interaction is significant only for a specific combination of optical phonons close to the zone center, i.e. the Fröhlich coupling is important only for a narrow distribution of wavevectors. The electron–phonon interaction involves thus two quasi discrete states and the strength of the interaction is larger than the energy width of the continuum. There is thus a strong coupling regime which leads to the formation of mixed electron–phonon quasiparticles called polarons. The eigenstates of the system are thus entangled states such as e.g. the P− polaron state $(\alpha \mid P-, 0 > + \beta \mid S, 1 >)$, i.e. linear combination of decoupled states $\mid a, n >$ where a corresponds to the electronic wave functions of the dots (S, P−, P+, . . .) and n corresponds to the number of coupled LO phonon modes. The existence of Rabi oscillations between electron and phonon components was first predicted by Inoshita and Sakaki in 1992 [9]. A clear signature of the effect of polaron formation was definitely reported by Hameau et al. by performing magneto-absorption measurements in resonance with the S-P transition of doped InGaAs quantum dots as a function of a strong magnetic field [10]. They did observe a strong deviation as compared to the magnetic field dependence of a parabolic confinement potential and this feature was fully taken into account by the developed polaron formalism.
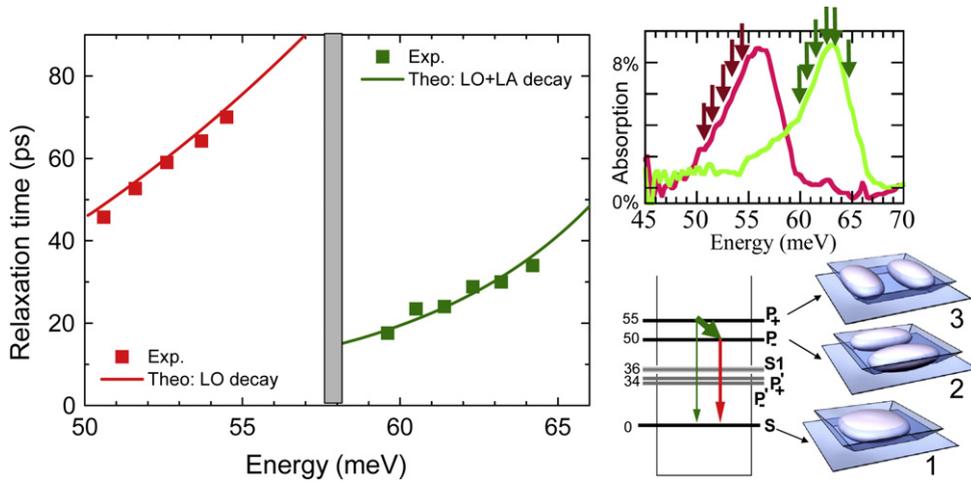
Fig. 3. Relaxation time dependence of the S-P− and S-P+ transitions as a function of the free electron laser few ps long pulse energy indicated by arrows in the absorption spectrum on the right. Relaxation paths are depicted by arrows in the schematic polaronic structure.

   The formation of polarons has a drastic influence on the quantum dot dynamics. At the beginning of the 1990s, a so-called phonon bottleneck in quantum dots was predicted based on energy conservation arguments [11]. This bottleneck which would translate in very long relaxation times was not experimentally observed either for intraband or interband relaxations. Optical saturation measurements performed at room temperature did report relaxation times in the picosecond range for bound-to-continuum transitions [12]. Pump-probe spectroscopy in resonance with the S-P transitions around 52 meV has shown that the relaxation time was in the tens of picosecond time scale. Fig. 3 shows the spectral dependence of the low temperature relaxation time measured for n-doped quantum dots [13]. The excitation is provided by the picosecond pulses of a free-electron laser tuned in resonance with the S-P intersublevel transition. The inhomogeneous broadening of the transition allows one to investigate the spectral dependence of the relaxation time with the same sample. The spectral width of the laser pulses is below 1 meV. The relaxation time is of the order of several tens of picosecond and increases as the polaron energy is further detuned from the LO phonon energy (36 meV for GaAs). These values are significantly larger than those which are measured in semiconductor quantum wells. One can observe that, even though the relaxation times are longer, there is no bottleneck for the intersublevel relaxation in quantum dots.

   This dependence can be fully understood using the polaron framework. It is well known that the phonons are unstable particles with a finite lifetime of a few ps. This instability is triggered by the lattice anharmonicities leading to the decay of LO phonons into a combination of acoustical or optical and acoustical phonons. The polarons being a combination of mixed states dressed with 0, 1, … phonons, it was first proposed by Li and co-workers using a semi-classical approach that the polaron lifetime should be dependent on the weight of the one phonon particle in the polaron eigenstate and that the polaron relaxation would be triggered by the instability and damping of the LO phonon component [14]. This semi-classical approach leads to the full line in Fig. 3 and provides a good agreement with the experimental results in the investigated spectral range. As seen, as the energy is detuned from the LO phonon energy, the relaxation time increases monotonously. Similar results have been obtained by Zibik and co-workers in 2004 [15]. The semi-classical model of Li et al. suffers however from a drawback: it predicts a continuous increase of the relaxation time at high energy. Experimental results have shown that this relaxation time can even decrease at energies higher than 56 meV, which correspond to the energy of a combination of two band-edge longitudinal acoustical phonons. It was recently shown by Grange and co-workers that the lifetime of the polarons at any energies can be correctly described by considering the polaron lifetime to be proportional to the LO phonon weight but that one needs to consider the different anharmonic decay channels not at the sole LO phonon energy but at the polaron energy [16]. Many different anharmonic channels involving different combination of phonons can indeed be involved in the polaron relaxation. Following this approach, the key elements which control the relaxation is not only the phonon weight but also the multiphonon density of states and the different anharmonic decay paths. This formalism explains that the polaron lifetime can decrease at energies higher than the two band-edge LA phonon energy. The same model also predicts a significant increase of the polaron lifetime at energies below the LO phonon energy. The

approach developed by Grange et al. thus provides a much more complete understanding of the quantum dot dynamics in the infrared range. We emphasize that the relaxation measurements discussed above only involve electron states and no holes are present in the structure. The presence of holes radically modify the polaron interaction and they also provide additional relaxation mechanisms through Auger transfer between the confined hole states.

4. Mid-infrared devices: towards quantum dot polaron lasers

The study of quantum dot dynamics has also revealed that an additional path exists between the P+ and P− energy-split states. An irreversible decay from the P+ state to the P− state can occur and be assisted in this case by acoustical phonons if the energy difference is not too large (few meV) [15]. The efficiency of the decay is strongly dependent on the energy splitting between both states. The efficiency of the interaction with acoustical phonons presents a maximum for wavevectors corresponding to the inverse of the quantum dot vertical size i.e. around 2 meV splitting. So the absolute values of the relaxation time are dependent on the quantum dot geometry. Above 2 meV splitting, the relaxation time increases when the detuning between P+ and P− increases. Typically, it is of the order of 20 ps for a 5 meV detuning and can be as small as 5 ps when the energy splitting between P− and P+ is 3 meV. The S, P− and P+ states can be considered as a three level system with a relaxation time from the P+ state which can be shorter than the relaxation time from the P− state. Like for the Ruby laser, it is thus possible to achieve a population inversion between P− and the S ground state, as long as the relaxation time from P+ to P− is shorter than the relaxation time from P− to S. This scheme, presented in Fig. 4, has been investigated theoretically by Sauvage and Boucaud in 2006 [17]. This modeling is based on the experimental measurement of the intersublevel absorption and on the experimental values of the polaron decay times as deduced from pump-probe experiments. The interest to study this system is manifold: first, the engineering of the relaxation rates between the polaron states could in principle lead to a first polaron laser. This engineering is based on the control of the polaron decay through the interaction with acoustical phonons and through the anharmonic instability of the polaron which depends on the weight $| \beta |^2$ of one optical phonon component in the polaron state $(\alpha \mid P-, 0 > + \beta \mid S, 1 >)$. Secondly, as the active transitions are based on in-plane polarized intersublevel transitions, normal incidence emission can be achieved. Third, the involved lifetimes are much longer than those between subbands in quantum cascade lasers. Another specific feature of intersublevel transitions are the long dephasing times that can be obtained. First measurements on quantum dot ensembles by optical Rabi oscillation have reported an already relatively long decay component characterized by a T2 time of several ps [18]. Recent measurements by Zibik and co-workers using four wave mixing have reported very long dephasing times in singly charged quantum dots limited only by the non-radiative T1 relaxation time, i.e. T2 can be as large as 100 ps for quantum dot intersublevel transitions [19]. These long dephasing and relaxation times translate at low temperature into a small saturation intensity. The optical gain that can be achieved in this system is shown in Fig. 4. A monomode waveguide structure was considered. The gain is dependent on the energy detuning between P+ and P− states. This energy detuning can be controlled during the growth of the sample or after growth by rapid thermal annealing. The gain can be as large as 300 cm^{-1} for a 3 meV detuning. As shown in Fig. 4, lasing can be achieved for a detuning up to 5 meV. The calculated threshold for an optical pump at 23 μm wavelength is around 1 kW·cm^{-2}. This threshold could be decreased by using other type of cavities instead of slab waveguides with cleaved facets like two-dimensional photonic crystals and by taking advantage of the reduced group velocities in these artificially-structured materials. For example, zone center Bloch modes at the Γ point of the Brillouin zone or defect cavity modes could be used to enhance the quality factors of the optical modes and decrease the threshold of polaron lasers. The next step is to experimentally obtain a laser effect which has not yet been reported.

5. Single quantum dot intersublevel absorption microscopy

All the results discussed so far were related to measurements made on quantum dot ensembles, and more generally on multilayer structures. A very significant trend over the last years in the quantum dot community has been the development of single dot studies based on interband transitions. The control at the single element level is very attractive for quantum manipulation of excitonic or spin states, generation of single photon or entangled photon pairs and can provide numerous perspectives for quantum information processing. One can therefore wonder if single quantum dot studies could also be performed using intersublevel transitions. Most of single quantum dot studies on interband transitions are based on photon emission. Unfortunately, the intersublevel emission is quite inefficient
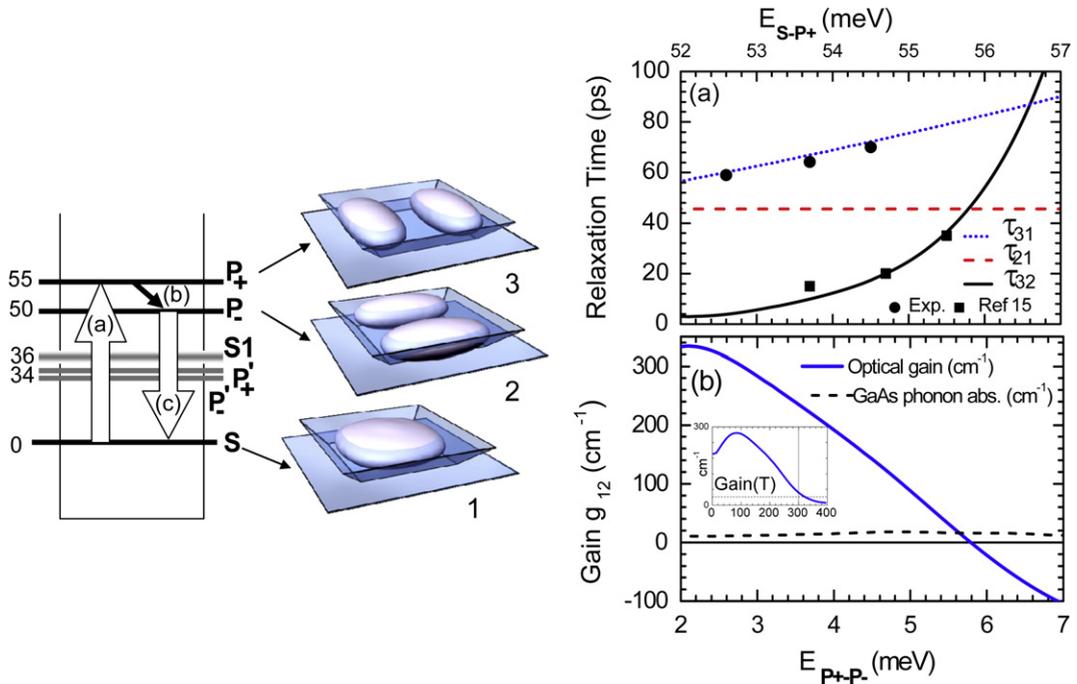
Fig. 4. Three level Ruby-like laser scheme based on polaron transitions in self-assembled InAs/GaAs quantum dots. Transition (a) is the pumping transition at 23 μm wavelength. Transition (b) is the fast relaxing transition between P+ and P−. Transition (c) is the lasing transition at 26 μm wavelength. Calculated relaxation times as a function of the P+-P− splitting are reported on the right-hand side for a fixed $E_{P−} = 50$ meV energy. The corresponding optical gain is reported below, as well as its temperature dependence for a splitting of 4 meV.

because of the fast non-radiative decays. For the S-P transition, the radiative lifetime is in the hundreds of nanosecond range while the non-radiative lifetime is in the tens of picosecond range. The measurement of spontaneous emission is thus quite challenging even for quantum dot ensembles. Note that the optical measurement of the absorption is also demanding. Because of the subsequent relatively larger homogeneous linewidths and long wavelengths, transmission variations measured in a diffraction limited setup are expected to be orders of magnitude smaller than in the interband case, in the 10^{-9}–10^{-6} range. This efficient non-radiative relaxation can however be considered as an asset instead of a drawback. The relaxation from an excited state is mainly followed by the emission of phonon wavepackets; this energy dissipation through phonon emission can thus be considered as a signature of the intersublevel absorption and the relaxation of carriers from excited states. We have recently developed a new set-up to probe this phonon emission at the local scale and by this way to detect the absorption of single quantum dots. The generation of phonon wavepackets can be detected at the sample surface by the tip of an atomic force microscope. Following an intersublevel absorption in a charged buried quantum dot, a thermal stress is generated and the strain field associated with phonon emission can propagate and diffuse towards the surface. Through a percussional excitation, the local stress transfers some energy to the cantilever of an atomic force microscope (AFM) which is in contact mode with the surface. The experimental set-up that we have developed can be viewed as a photo-acoustic and photo-thermal measurement with a local detection at the nanometer scale [20]. A schematic description of the experimental set-up is shown in Fig. 5. The optical excitation in resonance with the intersublevel absorption is provided by the picosecond pulses of a free-electron laser. The doped quantum dots are buried 20 nm below the surface. Following the absorption, the energy transferred to the cantilever by the surface displacement triggers the oscillation of the cantilever eigenmodes. This cantilever oscillation, which is in the tens of kHz range, can be detected with the alignment laser of the atomic force microscope. The measurement of this oscillation provides a local measurement at the nanometer scale of the surface deformation which results from the quantum dot absorption.

This technique provides a method to realize a two-dimensional imaging of single quantum dot absorption. Fig. 6 shows examples of two-dimensional images measured at room temperature for samples with different doping levels. The optical excitation is tuned in resonance with the S-D quantum dot intersublevel transition around 9.6 micron.
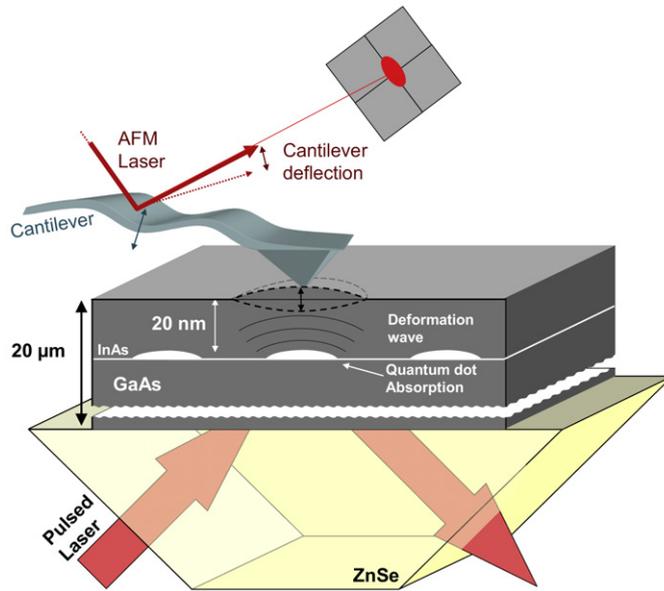
Fig. 5. Phonon detection scheme combining an atomic force microscope and a pulsed laser excitation. The AFM tip is in contact mode with the sample surface. The quantum dots are buried 20 nm beneath the surface. A fraction of the acoustic and thermal deformation energy is transferred to the cantilever leading to its slow mechanical oscillation, signature of the quantum dot absorption of the incident spectrally resonant laser pulses.
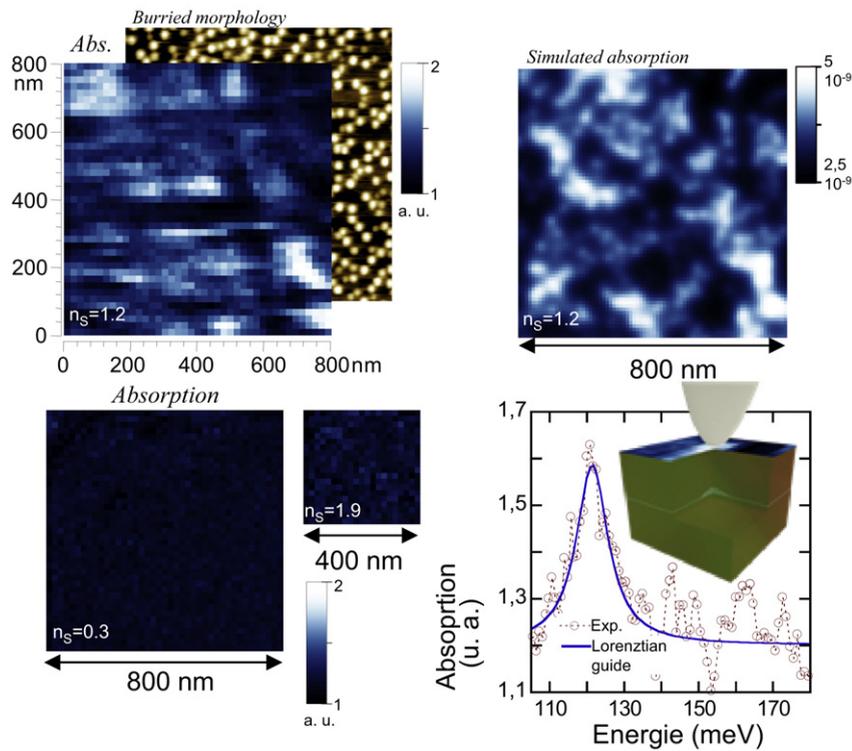

Fig. 6. Absorption microscopy and spectroscopy of single quantum dots at room temperature ($\lambda = 9.6$ μm). In the images the white spots correspond to the absorption of single quantum dots buried 20 nm beneath the surface. The cantilever energy is reported with a contrasted scale that goes from 1 (black) to 2 (white) for samples exhibiting various doping levels n_S as described in the text. The spectral dependence of the absorption is obtained by keeping the AFM tip fixed on top of a quantum dot and by varying the laser wavelength. The resonance is attributed to a S-D intersublevel transition.

The incident pulse energy is adjusted close to the saturation energy of the intersublevel absorption. The quantum dot density is 4×10^{10} cm^{-2} but all the dots are not significantly populated and all the populated quantum dots are not resonant with the exciting laser. The different doping levels are obtained by varying during the growth the nominal modulation doping. At room temperature, a strong thermoionic emission occurs and the samples need to be heavily doped in order to fully populate the quantum dot ground states. The different dopings correspond to a calculated average population n_S on the doubly degenerate dot ground states of 0.3, 1.2 and 1.9 carriers. The color scale follows the amplitude of the integrated signal around the 50 kHz resonance of the cantilever. The signal amplitude increases on top of an absorbing nano-object. For a weak quantum dot population n_S, the image contrast is almost uniform since the contribution of the quantum dots is masked by the residual background signal. For the sample with an average doping of 1.2 carrier per dot, the image has a significant contrast. A group of white pixels corresponds to the signature of the absorption of buried single quantum dots. Only few quantum dots are observed on the 800×800 nm^2 image whereas around 250 quantum dots are statistically buried under the surface. The spatial resolution for the absorption of a single quantum dot is around 60 nm (size of the white spots), i.e. well below the diffraction limit. At large doping densities, the contrast of the image vanishes since the free carriers which are uniformly distributed provide a significant contribution to the recorded signal. Note that a powerful feature of this approach is the possibility to perform localized spectroscopy by keeping the AFM tip fixed and by varying the laser wavelength. The resonance observed in the measured spectrum in Fig. 6 corresponds to one of the two allowed S-D transitions of a single quantum dot. These measurements using a photo-acoustic and photo-thermal measurement demonstrate that the intersublevel ultrasmall absorption of a single quantum dot can be measured even at room temperature and in the mid-infrared spectral range.

6. Conclusion

In conclusion, it is now well established that the physics of intersublevel transitions can be correctly described and understood in the framework of the polaron formalism. The key feature characterizing intersublevel transitions is the interplay between electronic states and phonons in quantum dots. The strong coupling with longitudinal optical phonons governs the quantum dot dynamics. For small energy splittings, the decay assisted by acoustical phonons can become predominant. The phonons are important to account for the electronic structure and dynamics. The energy released through phonon emission can be used as a signature of the intersublevel absorption. This feature has led to the detection at the nanometer scale of single quantum dot intersublevel absorption. Future work will concentrate on measurements at low temperature using this approach. Despite the striking advances reported over the last decade on intersublevel transitions, many open issues remain. Only very few works have been devoted to the intersublevel emission and the possibility to achieve lasing emission. The optical pumping with a three polaron level scheme is one route to demonstrate a first polaron laser. Many other approaches, using for example quantum dots embedded in quantum cascade structures, are being investigated. The coupling of intersublevel resonances with resonant modes of two-dimensional photonic crystals offers also many new opportunities to control the quantum dot emission. Finally, a new point of view is proposed, in which the quantum dots are not considered as natural photon sources but as natural phonon emitters. The quantum dots present a strong potential as localized acoustic nanosources and this aspect in combination with intersublevel excitations should emerge in the near future.

References

[1] H. Drexler, D. Leonard, W. Hansen, J.P. Kotthaus, P.M. Petroff, Spectroscopy of quantum levels in charge-tunable InGaAs quantum dots, Phys. Rev. Lett. 73 (16) (1994) 2252–2255.

[2] S. Sauvage, P. Boucaud, F.H. Julien, J.M. Gerard, V. Thierry-Mieg, Intraband absorption in n-doped InAs/GaAs quantum dots, Appl. Phys. Lett. 71 (19) (1997) 2785–2787.

[3] K.W. Berryman, S.A. Lyon, M. Segev, Mid-infrared photoconductivity in InAs quantum dots, Appl. Phys. Lett. 70 (14) (1997) 1861–1863.

[4] S. Sauvage, P. Boucaud, F.H. Julien, J.M. Gerard, J.Y. Marzin, Infrared spectroscopy of intraband transitions in self-organized InAs/GaAs quantum dots, J. Appl. Phys. 82 (7) (1997) 3396–3401.

[5] F. Bras, P. Boucaud, S. Sauvage, G. Fishman, J.M. Gerard, Temperature dependence of intersublevel absorption in InAs/GaAs self-assembled quantum dots, Appl. Phys. Lett. 80 (24) (2002) 4620–4622.

[6] P. Boucaud, S. Sauvage, Infrared photodetection with semiconductor self-assembled quantum dots, C. R. Physique 4 (10) (2003) 1133–1154.

[7] S. Sauvage, P. Boucaud, T. Brunhes, F. Glotin, R. Prazeres, J.M. Ortega, J.M. Gerard, Second-harmonic generation resonant with s-p transition in InAs/GaAs self-assembled quantum dots, Phys. Rev. B 63 (11) (2001) 113312.

[8] S. Sauvage, P. Boucaud, F. Glotin, R. Prazeres, J.M. Ortega, A. Lemaître, J.M. Gerard, V. Thierry-Mieg, Third-harmonic generation in InAs/GaAs self-assembled quantum dots, Phys. Rev. B 59 (15) (1999) 9830–9833.

[9] T. Inoshita, H. Sakaki, Electron relaxation in a quantum dot: Significance of multiphonon processes, Phys. Rev. B: Conden. Matter 46 (11) (1992) 7260–7263.

[10] S. Hameau, Y. Guldner, O. Verzelen, R. Ferreira, G. Bastard, J. Zeman, A. Lemaître, J.M. Gérard, Strong electron–phonon coupling regime in quantum dots: Evidence for everlasting resonant polarons, Phys. Rev. Lett. 83 (20) (1999) 4152–4155.

[11] H. Benisty, C.M. Sotomayor-Torres, C. Weisbuch, Intrinsic mechanism for the poor luminescence properties of quantum-box systems, Phys. Rev. B 44 (19) (1991) 10945–10948.

[12] S. Sauvage, P. Boucaud, F. Glotin, R. Prazeres, J.M. Ortega, A. Lemaître, J.M. Gerard, V. Thierry-Flieg, Saturation of intraband absorption and electron relaxation time in n-doped InAs/GaAs self-assembled quantum dots, Appl. Phys. Lett. 73 (26) (1998) 3818–3820.

[13] S. Sauvage, P. Boucaud, R.P.S.M. Lobo, F. Bras, G. Fishman, R. Prazeres, F. Glotin, J.M. Ortega, J.M. Gerard, Long polaron lifetime in InAs/GaAs self-assembled quantum dots, Phys. Rev. Lett. 88 (17) (2002) 177402.

[14] X.-Q. Li, H. Nakayama, Y. Arakawa, Phonon bottleneck in quantum dots: Role of lifetime of the confined optical phonons, Phys. Rev. B 59 (7) (1999) 5069–5073.

[15] E.A. Zibik, L.R. Wilson, R.P. Green, G. Bastard, R. Ferreira, P.J. Phillips, D.A. Carder, J.-P.R. Wells, J.W. Cockburn, M.S. Skolnick, M.J. Steer, M. Hopkinson, Intraband relaxation via polaron decay in InAs self-assembled quantum dots, Phys. Rev. B: Conden. Matter Mater. Phys. 70 (16) (2004) 161305.

[16] T. Grange, R. Ferreira, G. Bastard, Polaron relaxation in self-assembled quantum dots: Breakdown of the semiclassical model, Phys. Rev. B: Conden. Matter Mater. Phys. 76 (24) (2007) 241304.

[17] S. Sauvage, P. Boucaud, Intersublevel polaron laser with InAs/GaAs self-assembled quantum dots, Appl. Phys. Lett. 88 (6) (2006) 063106.

[18] F. Bras, S. Sauvage, G. Fishman, P. Boucaud, J.M. Ortega, J.M. Gerard, Fast decoherence of slowly relaxing polarons in semiconductor InAs quantum dots, Europhys. Lett. 70 (3) (2005) 390–396.

[19] E.A. Zibik, T. Grange, B.A. Carpenter, R. Ferreira, G. Bastard, N.Q. Vinh, P.J. Phillips, M.J. Steer, M. Hopkinson, J.W. Cockburn, M.S. Skolnick, L.R. Wilson, Intersublevel polaron dephasing in self-assembled quantum dots, Phys. Rev. B: Conden. Matter Mater. Phys. 77 (4) (2008) 041307.

[20] J. Houel, S. Sauvage, P. Boucaud, A. Dazzi, R. Prazeres, F. Glotin, J.-M. Ortega, A. Miard, A. Lemaître, Ultraweak-absorption microscopy of a single semiconductor quantum dot in the midinfrared range, Phys. Rev. Lett. 99 (21) (2007) 217404.